Valence quarks in the QCD plasma: quark number susceptibilities and screening

Rajiv V. Gavai[*] and Sourendu Gupta[†]

Department of Theoretical Physics, Tata Institute of Fundamental Research,

Homi Bhabha Road, Mumbai 400005, India.

Abstract

We have investigated the quark sector of quenched QCD for $1.5 \le T/T_c \le 3$ in the continuum limit, using two different lattice discretisations of quarks and extrapolating from lattice spacings between $1/4T$ and $1/14T$. At these temperatures, the flavour off-diagonal susceptibility, χ_{ud}/T^2, is compatible with zero at each lattice spacing, and hence also in the continuum limit. In the continuum limit, the light quark susceptibilities are about 10% less than the ideal gas results even at the highest T, in agreement with hard thermal loop predictions but marginally below a resummed perturbative computation. For the mass range appropriate to the strange quark, the flavour diagonal susceptibility is significantly smaller. Our estimate of the Wroblewski parameter is compatible with observations at RHIC and SPS. The continuum limit of screening masses in all (local) quark-bilinears is very close to the ideal gas results.

PACS numbers: 11.15.Ha, 12.38.Mh

---

[*]Electronic address: gavai@tifr.res.in

[†]Electronic address: sgupta@tifr.res.in

I. INTRODUCTION

Heavy-ion experiments at RHIC are now analysing large quantities of data and hope to identify and characterise the plasma phase of QCD. As a result it has become imperative to put together an accurate and detailed picture of this phase from theoretical analyses of QCD at finite temperature. Present day lattice computations are able to do a large part of this job. The reach of theory would certainly be enhanced if perturbation theory is tested accurately against these computations and, if found to work well, subsequently used in contexts where the lattice is too ponderous to use.

The gluon sector of the QCD plasma has been extensively analysed. In the quenched theory the scaling of T_c has been established to high accuracy [1, 2]. The continuum limit of the equation of state has also been determined to reasonably high accuracy [1, 3]. This shows strong departures from the ideal gas. It turns out that hard thermal loop (HTL) resummation is not sufficient for a description of the lattice results [4], nor is a Borel resummation of the perturbative series [5]. Other techniques such as an approximately self-consistent resummation [6] and dimensional reduction [7] have been applied, and the former has been successful in describing the lattice results for $T > 2T_c$. In addition, the spectrum of screening masses in the QCD plasma has been determined to good accuracy [8] and, for $T > 2T_c$, found to be in agreement with that determined non-perturbatively from a dimensionally reduced model whose couplings are matched perturbatively to the four-dimensional theory [9]. There is also direct evidence for the existence of the gluon as a quasiparticle in the plasma for $T > 1.5T_c$ [10].

The quark sector of the theory has not yet been explored in as much detail. Part of the reason is that lattice computations with light sea quarks are very expensive. While sea quarks are needed in the neighbourhood of the phase transition, where they influence even the order of the transition, sufficiently far away their effects are seen to be small [11, 12]. In this paper we report on the physics of valence quarks in the continuum limit of QCD for $T = 1.5T_c$–$3T_c$, where sea quark effects are marginal. The two aspects we concentrate on are quark number susceptibilities [13] and screening correlators and masses.

Quark number susceptibilities [11, 12, 13, 14, 15, 16] now occupy a position of high interest. Due to their connection with fluctuation phenomena [17] and strangeness production [15] they are useful inputs to relativistic heavy-ion collisions. They are coefficients of the

Taylor expansion of the free energy density of QCD in terms of the chemical potential, and hence are useful checks on recent attempts at numerical studies of finite-density QCD [18]. For exactly the same reason they are a test-bed for suggested resummations of the high-temperature perturbation series for QCD, which aim to reproduce the free energy density, and hence the equation of state, at high temperatures [19]. In this paper we report our study of these susceptibilities at a large variety of lattice spacings and an extraction of their continuum limit.

Screening correlators and masses are closely related to linear response functions such as susceptibilities. They have been explored earlier at finite lattice spacings, $1/4T$–$1/8T$. Staggered quarks were used in 4 flavour [20], 2 flavour [12, 21] and quenched [22, 23, 24] simulations. For reasons of symmetry a large degeneracy of screening masses, of the zero temperature scalar (S), pseudo-scalar (PS), and certain components of the vector (V) and axial-vector (AV) quark bilinears, is expected in the QCD plasma [27]. This was not observed; instead lesser degeneracies were— between parity partners S and PS or V and AV. Similar results were also obtained with overlap [25] and Wilson [26] quarks in quenched QCD, though the splitting between the S/PS and V/AV sectors was seen to be substantially smaller. Here we study these correlators on a wide range of lattice spacings and extrapolate the results to the continuum.

In this paper we carefully address the question of the continuum limit of these quantities in the quenched QCD plasma, where the valence quarks are used as probes of the dynamics of gluons. To this end we perform quenched computations over a range of temperatures and a large range of lattice spacings, in order to perform a continuum extrapolation. We test the extrapolation by working with two different formulations of quarks on the lattice, with different systematics at finite lattice spacing. One is the normal staggered formulation of quarks, the other a Symanzik improved version of staggered quarks, called Naik quarks [28]. By this means we identify a unique and verifiable continuum limit.

We would like to distinguish our approach from Symanzik (or loop level) improvement of the action [29]. Such programs aim to approach the continuum limit of the action on coarse lattices by adding terms to the action which systematically, order by order in the lattice spacing a, remove lattice artifacts up to some sufficiently high order in a. When such a scheme is used in conjunction with improved operators, it (ideally) obviates any need to go to very fine lattice spacings. In this work we only use an improved operator for the

valence quarks; the action is not improved. We reach the continuum limit by simulations on a variety of lattice spacings and a smooth extrapolation.

In the next section we present definitions of all the quantities that we measure, and results for these quantities for ideal quark gases on a lattice. In Section 3 we present details of the simulations and measurement schemes. The following section contains detailed results on the lattice with discussion of the extrapolation to the continuum. The continuum extrapolations are collected and discussed in the final section.

II. DEFINITIONS

The partition function of QCD with three quark flavours is

$$Z(T, \mu_u, \mu_d, \mu_s) = \int \mathcal{D}U \exp[-S(T)] \prod_{f=u,d,s} \det M(T, m_f, \mu_f), \tag{1}$$

where the temperature T determines the size of the Euclidean time direction, $S(T)$ is the gluon part of the action, and the determinant of the Dirac operator, M, contains as parameters the quark masses, m_f, and the chemical potentials, μ_f for flavours f. We also define the chemical potentials $\mu_0 = \mu_u + \mu_d + \mu_s$, $\mu_3 = \mu_u - \mu_d$ and $\mu_8 = \mu_u + \mu_d - 2\mu_s$, which correspond to the diagonal flavour $SU(3)$ generators. Note that μ_0 is the usual baryon chemical potential and μ_3 is an isovector chemical potential.

The quark number density for flavour f, n_f, is defined as the derivative of $F = \log Z/V$ (Z is the partition function and V the spatial volume) with respect to μ_f. The quark number susceptibilities are the second derivatives

$$\chi_{ff'}(T, \mu_u, \mu_d, \mu_s) = T \frac{\partial^2 F}{\partial \mu_f \partial \mu_{f'}}. \tag{2}$$

We will always drop the repeated subscript for the diagonal susceptibilities. There are similar susceptibilities, χ_0, χ_3 and χ_8 obtained by taking derivatives with respect to μ_0, μ_3 and μ_8 respectively. Here we determine the susceptibilities at $\mu_f = 0$. In this limit, all $n_f(T) = 0$ but the susceptibilities can be non-vanishing.

The flavour off-diagonal susceptibilities such as

$$\chi_{ff'} = \frac{T}{V} \left\langle \mathrm{tr} M_f^{-1} M_f' \, \mathrm{tr} M_{f'}^{-1} M_{f'}' \right\rangle \tag{3}$$

are given solely in terms of the expectation values of quark-line disconnected loops. Here M_f denotes the Dirac operator for a quark of flavour f, and M_f' and M_f'' the first and second

4

derivatives with respect to μ_f, taken term by term. The flavour diagonal susceptibilities have contributions from both quark-line connected and disconnected pieces—

$$\chi_f = \frac{T}{V}\left[\left\langle\left(\mathrm{tr}M_f^{-1}M_f'\right)^2\right\rangle + \left\langle\mathrm{tr}\left(M_f^{-1}M_f'' - M_f^{-1}M_f'M_f^{-1}M_f'\right)\right\rangle\right]. \tag{4}$$

We draw attention to the fact that the last two terms individually grow rapidly with lattice volume, diverging in the infinite volume limit, such that the difference is a finite quantity. This cancellation of divergences is the result of a proper treatment of quark chemical potentials on the lattice [30]. Numerically, the simplest quantity to evaluate is the diagonal isovector susceptibility

$$\chi_3 = \frac{T}{2V}\left\langle\mathrm{tr}\left(M_u^{-1}M_u'' - M_u^{-1}M_u'M_u^{-1}M_u'\right)\right\rangle, \tag{5}$$

where the factor half takes care of the isospin carried by each flavour. In addition to this, we shall need the baryon number and electric charge susceptibilities

$$\chi_0 = \frac{1}{9}\left(4\chi_3 + \chi_s + 4\chi_{ud} + 4\chi_{us}\right) \qquad \text{and} \qquad \chi_Q = \frac{1}{9}\left(10\chi_3 + \chi_s + \chi_{ud} - 2\chi_{us}\right). \tag{6}$$

Eqs. (3–5) have been written per flavour of quarks, *i.e.*, the normalisation for the continuum ideal gas is $\chi_f/T^2 = 1$.

The screening correlators of local quark-bilinear ("meson") operators are defined as—

$$C_\Gamma(z) = \sum_{x,y,t}\langle M_{\alpha\beta}^{-1}(x,y,z,t)\Gamma M^{\dagger}{}_{\beta\alpha}^{-1}(x,y,z,t)\Gamma\rangle \tag{7}$$

where Γ denotes some Dirac-flavour structure, α and β are colour indices and $M^{-1}(r)$ is the inverse of the Dirac operator for a point source in the fundamental of colour $SU(3)$ at the origin. Since the partition function of eq. (2) can be expressed as the trace of a spatial transfer matrix, the screening correlators decay exponentially, with characteristic length scales called screening lengths (inverse of screening masses, μ_Γ).

The finite temperature symmetries of such a spatial transfer matrix are quite different from that of the Hamiltonian and have been worked out in detail [27]. In particular, it turns out that there are only two independent local correlators. The combination of vector operators $V_x - V_y$ and axial vectors $AV_x - AV_y$ are in the B_1^{++} representation of the finite temperature symmetry group D_4^h. [35]. All others, *i.e.*, the scalar S, the pseudoscalar PS, and all the components of the V and AV orthogonal to the B_1^{++}, lie in the scalar representation,

5

A_1^{++}. This clearly implies that the angular momentum J is not a good quantum number for screening correlators, and hence states of different J can mix with each other.

The meson susceptibilities are the zero momentum part of the screening correlator [23] and can be written as

$$\chi_\Gamma \equiv \langle \mathrm{tr} M^{-1} \Gamma M^{-1} \Gamma \rangle = \sum_i Z_i(\Gamma) \left(\mu_\Gamma^i \right)^{-2}, \qquad \text{where} \qquad Z_i = \left| \langle i | \overline{\psi} \Gamma \psi | 0 \rangle \right|^2, \qquad (8)$$

$|i\rangle$ denotes the eigenstate of the transfer matrix with eigenvalue λ_i and the screening masses are $\mu_\Gamma^i = \log(\lambda_i/\lambda_0)$. In the continuum limit, since $M' = \gamma_0$, clearly $\chi_3 = \chi_{V_0}$; in fact, this identification underlies the computation of [19]. The PS susceptibility is also involved in a chiral Ward identity—

$$\langle \overline{\psi}\psi \rangle = m\chi_{PS}. \qquad (9)$$

At $T = 0$, chiral symmetry is broken and the sum over states in eq. (8) is dominated by the lowest term, due to the vanishing Goldstone pion mass. Then this Ward identity shows that $m_\pi^2 \propto 1/m$. However, for $T > T_c$, chiral symmetry is restored and $\langle \overline{\psi}\psi \rangle$ should vanish in the chiral limit. At the same time, χ_{PS} need not be dominated by one state and μ_{PS}^i could depend weakly on m, going to a finite non-zero limit as $m \to 0$. It is interesting to note that since the screening masses are equal for all the A_1^{++} channels, the differences between the susceptibilities can only come from the Z_i's in eq. (8).

For an ideal gas of quarks on the lattice, the Dirac operator at zero chemical potential is most simply written in momentum space where it is diagonal—

$$M_{pq} = \delta_{pq} \left[ma + i\gamma \cdot \hat{p} \right], \qquad \text{where} \qquad \hat{p}_\mu = C_{10} \sin p_\mu + C_{30} \sin 3p_\mu, \qquad (10)$$

the momentum spectrum is $p_0 = (2\pi/N_t)(n + 1/2)$ with $1 \le n \le N_t$ and $p_i = 2n\pi/N_i$ with $1 \le n \le N_i$ in all other directions, and $\hat{p}_\mu = \sin p_\mu$. For staggered quarks, where only a nearest neighbour difference appears in the Dirac operator, $C_{10} = 1/2$ and $C_{30} = 0$. For Naik quarks, on the other hand, $C_{10} = 9/16$ and $C_{30} = -1/48$. The construction of the number densities and conserved currents, and hence the chemical potential on the lattice, is complicated for Symanzik improved quarks, but goes through in the usual way [32].

All the quantities of interest are exactly computable for an ideal quark gas, not only in the continuum, but also on the lattice. In terms of $1/D(p) = (ma)^2 + \hat{p} \cdot \hat{p}$, $p'_\mu = -(C_{10} \cos p_0 + 3C_{30} \cos 3p_0)\delta_{0\mu}$ and $p''_\mu = (C_{10} \sin p_0 + 9C_{30} \sin 3p_0)\delta_{0\mu}$ we have—

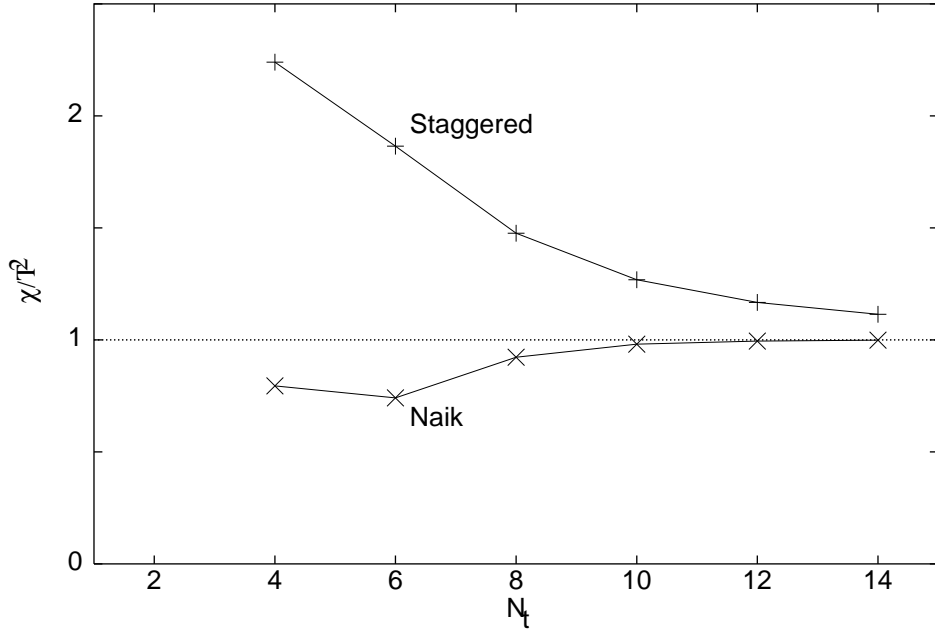$$a^3 \langle \overline{\psi}\psi \rangle_{FFT} = N_c \sum_p D(p),$$

FIG. 1: The ideal gas on a lattice with $TV^{1/3} = 3$ for staggered quarks (pluses) and Naik quarks (crosses), as a function of $N_t = 1/aT$.

$$a^2 \chi_{FFT} = \frac{N_c}{N_t N_s^3} \sum_p \left\{ D(p) \left[\hat{p} \cdot p' - p'' \cdot p'' \right] + 2D^2(p) \left(\hat{p} \cdot p'' \right)^2 \right\},$$

$$a\mu_{FFT}^{stag} = 2 \sinh^{-1} \sqrt{(ma)^2 + \sin^2(\pi/N_t)} \, . \qquad (11)$$

Figure 1 shows the susceptibilities for the staggered and Naik quarks on a sequence of lattices with fixed aspect ratio $N_s/N_t = 3$. Note that the approach to the continuum limit is quite different in the two cases. In free-field theory $\chi_{ud} = 0$. The computation of the correlators $C_\Gamma(z)$ in the ideal gas is also straightforward. Perturbative expansions in the gauge coupling, g, have been performed in the continuum. χ_3 has been computed in the hard thermal loop (HTL) approximation to order g^3 as well as in a skeleton graph resummation [19]. To the best of our knowledge, there has been no such computation of screening correlators, screening masses or the remaining susceptibilities.

N_t	1.5T_c			2T_c			3T_c		
	β	V	Stats	β	V	Stats	β	V	Stats
4	5.8941	12^3	$50 \times \mathbf{51}$	6.0625	12^3	$50 \times \mathbf{50}$	6.3384	16^3	$50 \times \mathbf{28}$
6	6.0625	20^3	$1000 \times \mathbf{54}$	6.3384	20^3	$1000 \times \mathbf{55}$	6.7	20^3	$1000 \times \mathbf{59}$
8	6.3384	18^3	$1000 \times \mathbf{57}$	6.55	18^3	$100 \times \mathbf{54}$	6.95	26^3	$500 \times \mathbf{30}$
		32×18^2	$100 \times \mathbf{47}$		32×18^2	$100 \times \mathbf{20}$		32×26^2	$100 \times \mathbf{20}$
10	6.525	22^3	$50 \times \mathbf{105}$	6.75	22^3	$50 \times \mathbf{219}$	7.05	32^3	$50 \times \mathbf{23}$
		40×22^2	$100 \times \mathbf{20}$		40×22^2	$100 \times \mathbf{20}$		40×32^2	$100 \times \mathbf{20}$
12	6.65	26^3	$50 \times \mathbf{75}$	6.90	26^3	$50 \times \mathbf{173}$	7.20	38^3	$50 \times \mathbf{50}$
		48×26^2	$100 \times \mathbf{24}$		48×26^2	$100 \times \mathbf{61}$		48×38^2	$100 \times \mathbf{20}$
14				7.00	30^3	$1000 \times \mathbf{48}$			

TABLE I: The lattice sizes, $N_t \times N_s^3$, Wilson coupling, β, and statistics used in this study. The statistics is reported as $N_{sep} \times \mathbf{N}_{stat}$ where N_{sep} is the number of sweeps between measurements and $\mathbf{N}_{stat}$ is the number of measurements. 1000 initial sweeps were discarded for thermalisation in all cases except the $N_t = 14$ run, where 7000 sweeps were discarded. For asymmetric spatial sizes the long direction is called the z-direction.

III. METHODS

As already mentioned, we have investigated quark number susceptibilities using two different realisations of lattice quarks. For staggered quarks, the derivative in the Dirac operator is discretised using a one-link separated finite difference operator. This has a discretisation error of order a^2. The improvement suggested by Naik [28] is to take a specific three-link term (see eq. 10) which cancels the leading term of the discretisation error for staggered Fermions up to $\mathcal{O}(a^3)$. This possible improvement comes at a fourfold increase in computational cost, due to the more complicated structure of the Dirac operator.

Since the discretisation error in the evaluation of the susceptibilities comes partly from the gauge action and partly from the Dirac operator, and we use the Wilson gauge action, the part of the $\mathcal{O}(a^2)$ error coming from this source would remain the same in the two determinations. However, if a large part of the $\mathcal{O}(a^2)$ error in the determination of susceptibilities using staggered quarks comes from the traces of the Dirac operator in eqs. (3–5), then the

slope in the extrapolation to the continuum limit should be substantially different between the two quark formulations. That this is so can be seen already in the computation for the ideal quark gas, illustrated in Figure 1.

In this paper we report results on susceptibilities and screening measured on lattices with $4 \leq N_t \leq 14$ for $T = 1.5T_c$, $2T_c$ and $3T_c$. The lattices sizes, couplings and statistics used are reported in Table I. Due to statistical errors in the determination of critical couplings various other quantities that go into a scale determination, the temperature corresponding to a given lattice coupling may be in error by about 5% [27]. The simulations have been performed with a Cabbibo-Marinari pseudo-heatbath technique with 3 $SU(2)$ subgroups updated on each hit, each sweep consisting actually of 5 sweeps of this algorithm. For susceptibilities we have made measurements using both staggered and Naik quarks at $m/T_c = 0.1$, 0.5 and 1. For staggered quarks we have also used $m/T_c = 0.03$. For screening masses and correlators we have used only staggered quarks.
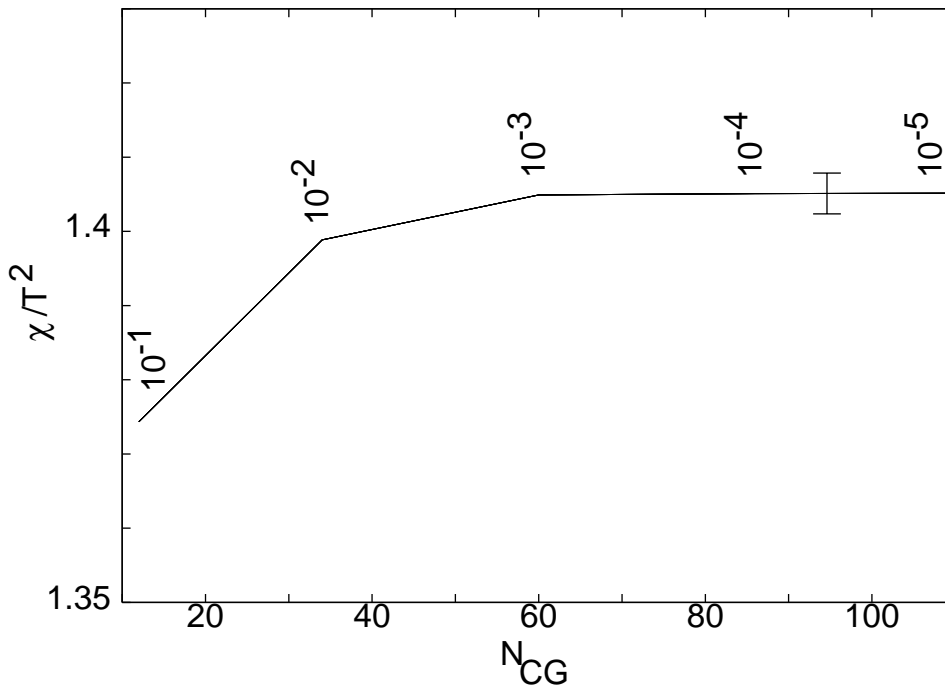

FIG. 2: The variation of the estimate of χ_3/T^2 on a single configuration with N_{CG}, which values as $\ln(1/\epsilon_{CG})$. The values of ϵ_{CG} are marked at appropriate points on the curve. The size of typical errors on the estimates, after averaging over 50 gauge configurations with $N_v = 10$, is shown as the bar. This is insensitive to ϵ_{CG}.

The stochastic evaluation of traces depends on the identity

$$\mathcal{I}_{\alpha\beta} = \frac{1}{2N_v} \sum_{i=1}^{N_v} R_i^\alpha (R_i^*)^\beta,\tag{12}$$

where $\mathcal{I}$ is the identity matrix, R_i^α is the component α of the vector R_i, which is one of a set of N_v uncorrelated vectors with complex components drawn independently from a Gaussian ensemble with unit variance, and the star denotes complex conjugation. This leads to the stochastic estimators,

$$\text{Tr}\,A = \text{Tr}\,A\mathcal{I} = \frac{1}{2N_v} \sum_{i=i}^{N_v} R_i^\dagger A R_i. \qquad (\text{Tr}\,A)^2 = \text{Tr}A\mathcal{I}A\mathcal{J}\tag{13}$$

where the vectors used in the stochastic estimators of the two identity matrices, $\mathcal{I}$ and $\mathcal{J}$, are different. This is done by dividing the set of R_i into disjoint blocks.

It turns out that the divergence cancellation in eq. (5) is numerically the hardest part of the computation. In previous works we had taken a half-lattice version of the staggered Dirac operator, which performed extremely well on small lattice volumes but was inefficient at divergence cancellation on large volumes [15], leading to enormous statistical fluctuations. We found that the full lattice version of the staggered Dirac operator performs much better in this respect, and has no trouble handling our largest lattices. The statistical fluctuations are under good control already with $N_v = 10$, and one has no need to look for reduced variance versions of eq. (12). We found that it is important to work in that sector of the quenched theory in which the Wilson-Polyakov line, L, is purely real. This can always be achieved by a Z_3 rotation in the quenched theory.

The slowest part of the computation is the inversion of the Dirac operator, M, which is done by a conjugate gradient iteration. The time taken is linear in the number of iterations, N_{CG}. This in turn depends on the precision required in the solution, which is specified by a single number ϵ_{CG} through the requirement that $|Mx - r|^2 \le N_t V \epsilon_{CG}$ (here r is one of the random vectors and x is the estimate of $M^{-1}r$). In Figure 2 we show how the estimate of χ_3/T^2 changes with $N_{CG} \propto \log(1/\epsilon_{CG})$. It is clear that with $\epsilon_{CG} = 10^{-3}$ the result is statistically indistinguishable from that with $\epsilon_{CG} = 10^{-5}$, but the solution is achieved at half the CPU cost. We have used $\epsilon_{CG} = 10^{-3}$ in all our computations of χ. It turns out that the estimation of screening correlators is more sensitive to the stopping criterion, requiring $\epsilon_{CG} = 10^{-5}$.

The fits and fit errors involved in the continuum extrapolations are done by a bootstrap method. In this, bootstrap samples of the data are extracted and fits are performed on statistics obtained from each such sample. The statistics of the fitted parameters are then used to obtain non-parametric estimators of the mean and variance. We have varied the number of bootstrap samples by two orders of magnitude, between 10 and 1000, to check that the estimators are stable.

We have used staggered quarks to determine screening correlators and masses. Recall the well-known fact that for these, the one link transfer matrix contains complex eigenvalues and leads to oscillations in the screening correlators. However, the two link transfer matrices have real eigenvalues, and the corresponding states can be projected by a simple parity projection. Due to the three-link terms in the Naik Dirac operator, real eigenvalues are obtained only for the four-link transfer matrix. The one link transfer matrix contains oscillatory mixtures of various states from which pure states need to be projected out. We show in the next section that we can reach the continuum limit with staggered quarks. Since they lead to simpler correlators, we have analysed screening phenomena only with these. We have concentrated on degeneracies of the screening correlators as well as the screening masses. The latter were extracted from local masses as well as by making two-mass fits to the parity projected correlators. Details of these techniques remain the same as in [12]. For bias-free extraction of screening masses, large separations in the spatial directions are necessary. Consequently, we have only used data from lattices with $N_z = 4N_t$ for this analysis (see Table I).

IV. LATTICE RESULTS

As shown in Figure 1 an ideal gas of staggered quarks has strong lattice artifacts and one needs lattices with $N_t \simeq 8\text{--}12$ in order to get continuum results. Computations in quenched QCD, shown in Figure 3 also indicate this. Note specially that for $N_t = 4$ and 6, χ_3/χ_{FFT} decreases with N_t at fixed T, unlike at larger N_t where it increases. This means that with staggered quarks one needs fairly fine lattices for a smooth extrapolation to the continuum.

Unfortunately, Naik quarks also have their own quirks. An ideal gas of Naik quarks on a lattice approaches the continuum smoothly only for $N_t > 6$ as shown in Figure 1. The interacting theory also exhibits departures from smoothness, as shown in Figure 3. At $1.5T_c$ it might seem that the $N_t = 6$ and 8 lattices scale, but at $2T_c$ this scaling is seen to be

N_t	1.5T_c			2T_c			3T_c		
	Staggered		Naik	Staggered		Naik	Staggered		Naik
	0.03	0.1	0.1	0.03	0.1	0.1	0.03	0.1	0.1
4	1.816 (16)		1.112 (22)	1.846 (6)		1.137 (14)	1.911 (5)		1.114 (15)
6*	1.312 (59)		0.957 (36)	1.428 (5)	1.425 (5)	1.033 (14)	1.492 (4)		0.993 (10)
8	1.110 (11)	1.105 (11)	0.936 (9)	1.144 (11)	1.142 (11)	0.952 (8)	1.191 (19)	1.190 (19)	0.979 (5)
10	1.014 (6)	1.009 (6)	0.921 (7)	1.060 (8)	1.058 (8)	0.948 (4)	1.066 (7)	1.066 (7)	0.956 (7)
12	0.973 (14)	0.969 (14)	0.915 (7)	0.994 (7)	0.992 (7)	0.941 (9)	1.027 (6)	1.026 (6)	0.950 (5)
14				0.985 (10)		0.949 (2)			

TABLE II: Lattice results for χ_3/T^2, with $m/T_c = 0.03$ and 0.1 for staggered quarks and 0.1 for Naik quarks. For $N_t = 6$ the three temperatures are 1.33T_c, 2T_c and 3.13T_c.
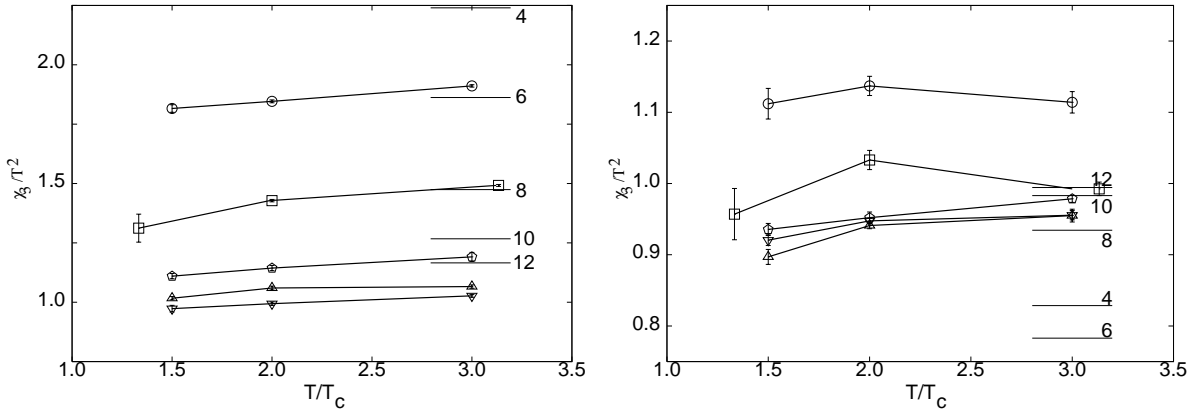

FIG. 3: The temperature dependence of χ_3/T^2 with staggered (left panel) and Naik (right panel) quarks of masses 0.03T_c and 0.1T_c respectively, with $N_t = 4$ (circles), 6 (boxes), 8 (pentagons), 10 (down triangles) and 12 (up triangles). Note the differences in the y-axes in the two cases. The bold lines join the centers of the data points. The thin lines show the value of χ_3/T^2 for an ideal gas on the same lattices at 3T_c.

accidental. In turn, at 2T_c one sees $N_t = 8$, 10 and 12 as scaling, but at 3T_c this turns out to be accidental.

Our results for χ_3/T^2 obtained with staggered and Naik quarks for the lightest quark masses are collected in Table II. In Figure 4 we show the extrapolation of staggered and

Naik quark results on χ_3 at $T = 2T_c$ to the continuum limit. For staggered quarks only the data for $N_t \geq 8$ fits a simple quadratic extrapolation of the form $\chi_3(a)/T^2 = \chi_3/T^2 + s/N_t^2$ [36]. In fact, for smaller N_t the extrapolations of χ_3/χ_{FFT} even gives the wrong sign for s [37]. However, for $N_t \geq 8$ the extrapolations of χ_3/T^2 and χ_3/χ_{FFT} give identical results. Since the two ratios reach this limit from different directions, their agreement is already a good indicator of having the right continuum limit. For Naik quarks at $2T_c$, the quadratic extrapolation looks reasonable for $N_t \geq 4$. This is accidental; at $3T_c$ or at $1.5T_c$ a good fit is obtained only for $N_t \geq 6$. Furthermore, as already mentioned, the extrapolation of χ_3/χ_{FFT} for Naik quarks does not coincide with that of χ_3/T^2 even at the 3-σ level. The extrapolation of χ_3/T^2 does, however, agree within errors with the continuum extrapolation from staggered quarks.

We reiterate the following point. In this quenched work with the Wilson action we have taken staggered and Naik quarks to provide two different operators to measure the same
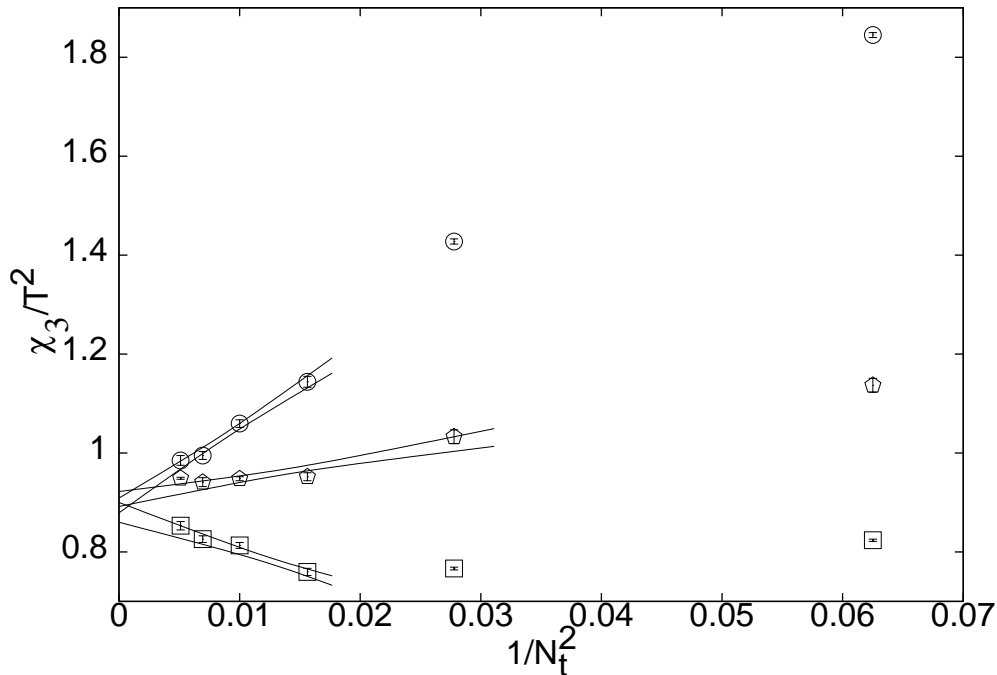

FIG. 4: The continuum extrapolation of staggered and Naik quark data for χ_3 at $2T_c$. The circles are the extrapolation of χ_3/T^2 for staggered quarks, the boxes for χ_3/χ_{FFT} for staggered quarks, and the pentagons for χ_3/T^2 for Naik quarks. The bands are 1–σ error bands for an extrapolation in $a^2 \propto 1/N_t^2$.
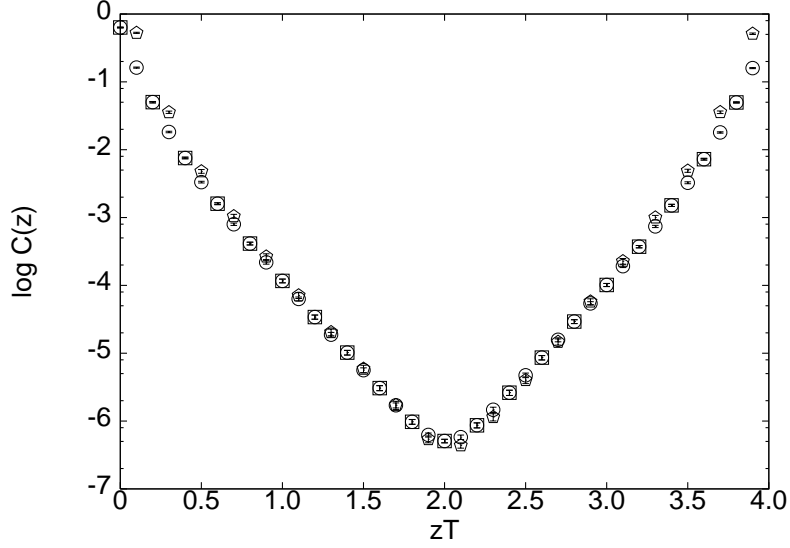
FIG. 5: The parity projected screening correlators evaluated with staggered quarks of mass $0.03T_c$ at $T = 2T_c$. The degeneracy of PS (circles) and S (boxes) correlators is evident, as is the equality of the screening masses for these and the V (pentagons) correlator. The S and PS correlators are divided by 3 to bring them into coincidence with the V. The other A_1^{++} correlators, which are not shown, are also in equally good agreement with these.
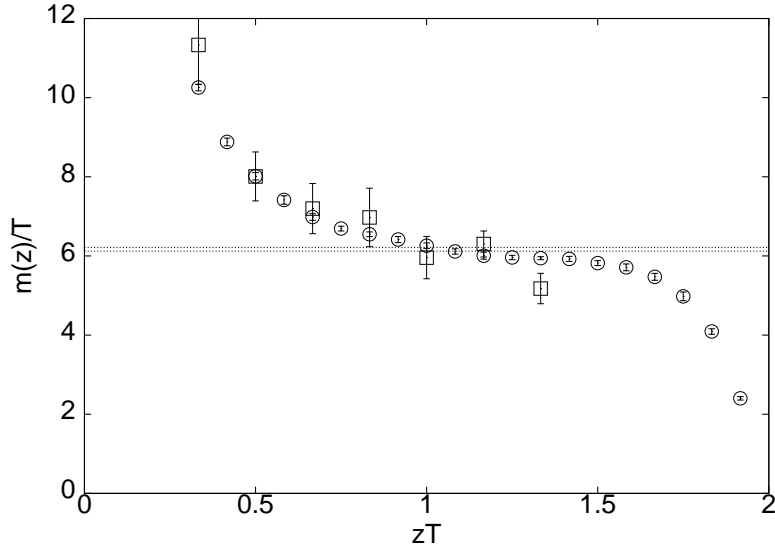

FIG. 6: Local masses for the PS correlator (circles) compared with the result of a two-mass fit. The data are for a $12 \times 48 \times 26^2$ lattice at $2T_c$ with $m = 0.03T_c$ for staggered quarks. Also shown are local masses for the V correlator (boxes) in the A_1^{++} representation.

14

N_t	$1.5T_c$	$2T_c$	$3T_c$
4	4.12 (12)	4.576 (16)	
6		5.34 (6)	
8	5.536 (24)	5.744 (32)	5.928 (64)
10	5.67 (2)	6.07 (4)	6.04 (10)
12	5.904 (96)	6.156 (48)	6.156 (180)

TABLE III: A_1^{++} local masses for staggered quarks with $m = 0.03T_c$.
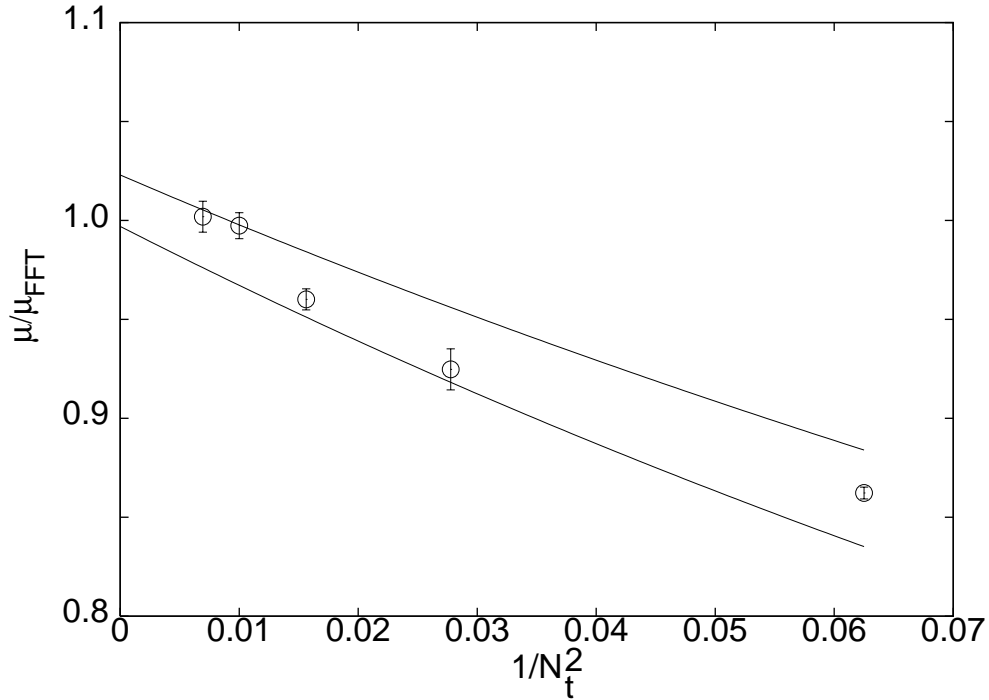

FIG. 7: Extrapolating the ratio of the measured A_1^{++} screening mass, μ_{PS}/T, and its value in an ideal quark gas to the continuum limit. The data are for $T = 2T_c$ and $m = 0.03T_c$ for staggered quarks. Already at lattice spacings $a = 1/10T$ and greater the result is compatible with unity.

physical quantity, namely χ_3. The agreement between the two provides a check that we have control over the continuum limit. In this approach we find that equally small lattice spacings are needed for the two kinds of quarks, and therefore Naik quarks are fourfold more time consuming. The use of improved actions to get continuum results with coarse lattices is a different problem. Our observations do not rule out the possibility that improved gauge
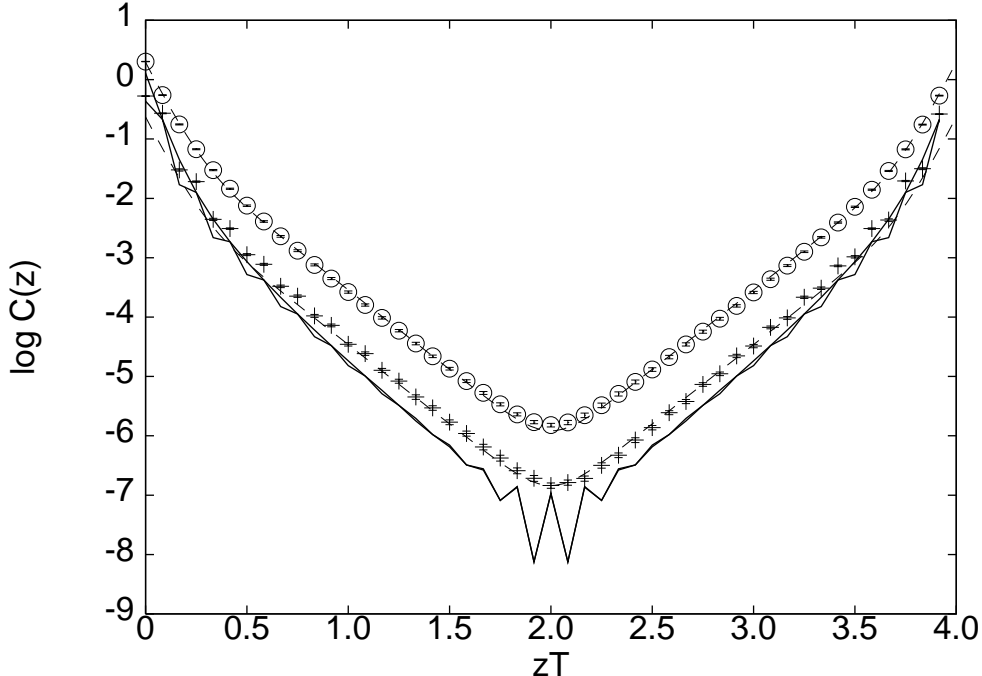
FIG. 8: The A_1^{++} screening correlators in the PS (circle) and unprojected V (pluses) channels compared to their ideal gas counterparts (heavy lines) for staggered quarks. These were determined on $12 \times 26^2 \times 48$ lattices at $T = 2T_c$ with staggered quarks of $m = 0.03T_c$. The best fit to the PS data is shown (broken line) as is the same fit multiplied by an overall constant to superpose it on the data for V, in order to show that these two correlators give the same screening mass. Note that the short distance part of the V correlator agrees rather well with the ideal gas expectation, unlike the PS correlator which differs by a factor two.

actions with fat link dynamical Naik quarks approach the continuum action more rapidly and that with such actions fat link Naik quark operators have smoother approach to the continuum already at coarser lattice spacings.

The off-diagonal susceptibility, χ_{ud}/T^2, is consistent with zero at 95% confidence level on all the lattice sizes, couplings and masses investigated, and at the 67% level on most. The extrapolation to the continuum of χ_{ud}/T^2 can be performed by the same functional form as for χ_3/T^2, and, unsurprisingly, gives a result consistent with zero for both staggered and Naik quarks. For the strange quark mass region also, similar results are obtained. In view of these, we neglect the quark-line disconnected amplitudes in all the susceptibilities in eq. (6). The continuum results for χ_s/T^2, χ_0/T^2 and χ_Q/T^2 are discussed in the next section.

16

We have seen clear degeneracies of the S and PS correlators and the V and AV correlators— in agreement with all previous observations. The new result is that with sufficiently fine lattices spacings, i.e., $a = 1/8T$–$1/12T$, we find a degeneracy of the A_1^{++} masses from the S/PS correlators and the V/AV correlators. In Figure 5 we demonstrate this by showing that the S/PS correlators are coincident with the V/AV correlators up to a constant multiplicative factor.

The local masses plateau for distances $z > 1/T$ and agree with the results of the fit. An example is shown in Figure 6. The result of a two mass fit to the PS correlator coincides within errors with the plateau in the local masses. Also, the local masses from the parity projected A_1^{++} components of the V/AV correlators coincide with those from the S/PS correlators. Our estimates of the common mass are collected in Table III.

For $a = 1/4T$ our extraction of μ_{PS}/T is completely consistent with previous estimates; for example, $a\mu_{PS} = 1.144$ (4) at $T = 2T_c$, in perfect agreement with the results of [23]. However, with decreasing lattice spacing we find that μ_{PS} increases rapidly toward the values expected for an ideal quark gas, eq. (11). In Figure 7 we show μ_{PS}/μ_{FFT} as a function of $1/N_t^2 \propto a^2$. Already for $a = 1/10T$ the screening mass is completely consistent with that in an ideal gas. It can be seen that a quadratic extrapolation to the continuum limit at $2T_c$ is consistent with an ideal quark gas. At all three temperatures we see clear degeneracy of all the A_1^{++} screening masses on the larger lattices. The B_1^{++} correlators vanish within errors even on the coarsest lattice [31]. This behaviour is also compatible with expectations from an ideal quark gas.

Interestingly, the measured values of $\langle \overline{\psi}\psi \rangle$ differ from the ideal gas value by a factor of about two on all the lattices studied. Within statistical errors $\langle \overline{\psi}\psi \rangle$ is independent of volume, and its ratio to the ideal gas value has small lattice spacing dependence, extrapolating smoothly to 1.90 ± 0.04 at $2T_c$ in the continuum. In view of the chiral Ward identity of eq. (9) which relates the pion correlator to the chiral condensate, and the agreement of the screening masses with their ideal gas values, we examine the screening correlators for the origin of this major departure from ideal gas behaviour. In Figure 8 are shown the PS and V screening correlators at $T = 2T_c$ obtained with lattice spacing $a = 1/12T$. It is clear that the correlators are significantly different from their ideal gas counterparts, not just in an overall factor (which would be sufficient to explain the chiral condensate) but also in shape.
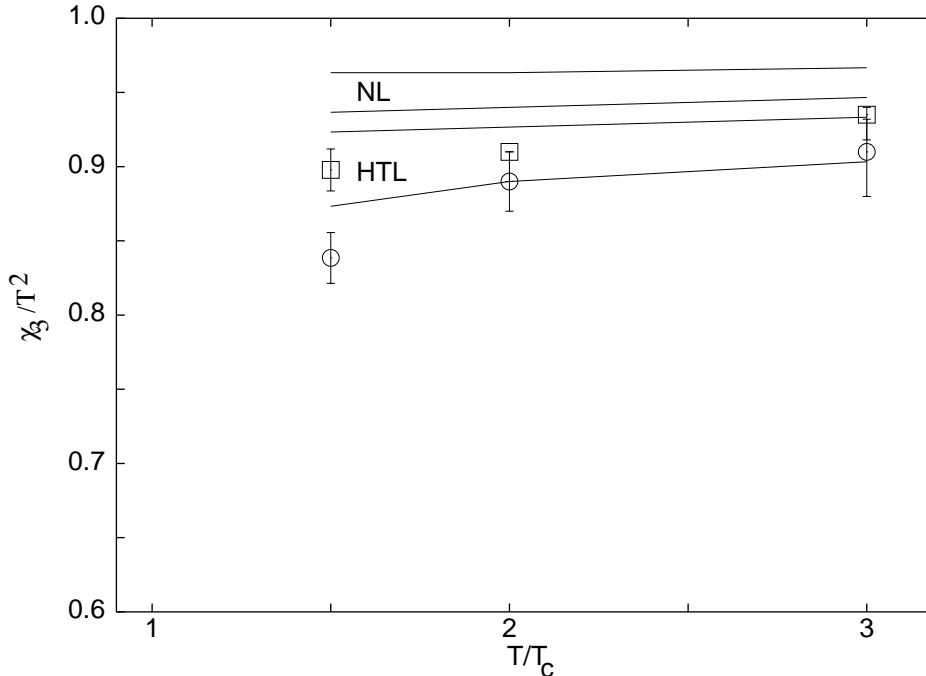
FIG. 9: The ratio χ_3/χ_{FFT}^3 in quenched QCD, shown as a function of T. Circles denote results for staggered quarks and boxes for Naik quarks. Also shown are the hard thermal loop (HTL) and resummed (NL) results from [19]. The bands for the last two are due to uncertainties in $T_c/\Lambda_{\overline{MS}}$.

V. CONTINUUM PHYSICS

Our results for the dependence of the continuum extrapolated values of χ_3/T^2 on T/T_c are shown in Figure 9. We find that the results obtained with staggered and Naik quarks are compatible with each other and with the HTL results of [19] at the 2–σ level. While they are not compatible with the resummed results of [19] at the 1–σ level, compatibility cannot be ruled out at the 3–σ level for $T \geq 2T_c$. There is a suggestion of a drop in χ_3/T^2 as one approaches T_c. In Table IV we have listed the continuum extrapolated values of χ_3/T^2 and χ_{ud}/T^2 along with the susceptibilities χ_s/T^2, χ_0/T^2 and χ_Q/T^2 which are of relevance to heavy-ion experiments.

Previous lattice investigations at cutoff of $1/4T$ have shown that the effect of unquenching is to increase χ_3/T^2 by less than 5% [11, 12]. The computations of [19] indicate that the effect of unquenching is to decrease χ_3/T^2 by less than 5%. Thus the effect of including light sea quarks could change the results in Table IV either way within a band of 3–5%.

T/T_c	χ_3/T^2	χ_{ud}/T^2	χ_s/T^2	χ_0/T^2	χ_Q/T^2	$\lambda_s(T)$	$\mu(A_1^{++})/2\pi T$
1.5	0.84 (2)	$(-2 \pm 3) \times 10^{-5}$	0.53 (1)	0.43 (1)	0.99 (2)	0.63 (3)	0.96 (1)
2.0	0.89 (2)	$(-4 \pm 4) \times 10^{-6}$	0.71 (2)	0.47 (1)	1.07 (2)	0.80 (3)	1.01 (1)
3.0	0.90 (3)	$(2 \pm 2) \times 10^{-6}$	0.84 (3)	0.49 (1)	1.09 (3)	0.93 (4)	1.00 (1)

TABLE IV: Results for the continuum limit of quark number susceptibilities, the Wroblewski parameter, $\lambda_s(T)$, expected of a system at thermal equilibrium at temperature T, and the A_1^{++} screening mass in quenched QCD. We have taken $m_s/T_c = 1$, as appropriate to full QCD. All the values reported in this table have been obtained by continuum extrapolation of our staggered quark results. Those from Naik quarks are compatible within 1–σ limits, except for χ_3 at $T = 1.5T_c$ which agrees within 95% confidence limits.

The Wroblewski parameter [33], λ_s, measures the ratio of primary produced strange to light quark pairs. It has been argued [15] that, for a system undergoing freeze out from thermal and chemical equilibrium at temperature T, λ_s is just the ratio $2\chi_s/(\chi_u + \chi_d)$ computed at T. We have listed the continuum values of $\lambda_s(T)$ obtained from our lattice simulations in Table IV. Note especially that $\lambda_s(T)$ for the staggered and Naik quarks are within 1–σ of each other. Various extrapolations of $\chi_u = \chi_d$ and χ_s yield $\lambda_s(T_c) \approx 0.4$–0.5. It seems plausible that at $T \approx T_c$, λ_s dips toward the value obtained from analysis of RHIC data, *i.e.*, 0.47 ± 0.04 [34].

Table IV also contains our determination of the common screening mass in the A_1^{++} sector for light quarks. At temperatures of $2T_c$ and higher this is completely compatible with a computation in an ideal gas. Similarly, χ_{ud}/T^2 is also compatible with expectations from an ideal gas. It has been pointed out before that χ_{ud}/T^2 is significantly smaller than might be expected in the leading perturbative treatment of the interactions. In future it would be interesting to investigate perturbative corrections to the screening masses and check whether a similar puzzle exists also for them, or whether interaction effects indeed are smaller than the error bars on these quantities. Departures from ideal gas behaviour, by a factor of almost two, has been observed in the chiral condensate, and hence in the PS susceptibility. It would

be useful to have perturbative predictions for these quantities in the future.

[1] G. Boyd *et al.*, *Nucl. Phys.*, B 469 (1996) 419.

[2] S. Gupta, *Phys. Rev.*, D 64 (2001) 034507.

[3] C. Bernard *et al.*, *Phys. Rev.*, D 55 (1997) 6861. J. Engels *et al.*, *Phys. Lett.*, B 396 (1997) 210; A. Ali Khan *et al.*, *Phys. Rev.*, D 63 (2001) 034502, *ibid.*, D 64 (2001) 074510.

[4] J. O. Andersen, E. Braaten and M. Strickland, *Phys. Rev.*, D 61 (2000) 014017, *ibid.*, D 61 (2000) 074016; J. O. Andersen *et al.*, hep-ph/0205085.

[5] R. Parwani, *Phys. Rev.*, D 63 (2001) 054014, *ibid.*, D64 (2001) 025002.

[6] J.-P. Blaizot, E. Iancu and A. Rebhan, *Phys. Rev. Lett.*, 83 (1999) 2906.

[7] K. Kajantie *et al.*, *Phys. Rev. Lett.*, 86 (2001) 10.

[8] S. Datta and S. Gupta, *Nucl. Phys.*, B 534 (1998) 392 and hep-ph/9809382; S. Datta and S. Gupta, *Phys. Lett.*, B 471 (2000) 382.

[9] A. Hart, M. Laine and O. Philipsen, *Nucl. Phys.*, B 586 (2000) 443.

[10] S. Datta and S. Gupta, hep-lat/0208001.

[11] R. V. Gavai and S. Gupta, *Phys. Rev.* D 64 (2001) 074506.

[12] R. V. Gavai, S. Gupta and P. Majumdar, *Phys. Rev.*, D 65 (2002) 054506.

[13] S. Gottlieb *et al.*, *Phys. Rev. Lett.* 59 (1987) 2247.

[14] R. V. Gavai *et al.*, *Phys. Rev.* D 40 (1989) 2743; C. Bernard *et al.*, *Phys. Rev.* D 54 (1996) 4585; S. Gottlieb *et al.*, *Phys. Rev.*, D 55 (1997) 6852.

[15] R. V. Gavai and S. Gupta, *Phys. Rev.*, D 65 (2002) 094515.

[16] C. Bernard *et al.*, hep-lat/0209079.

[17] M. Asakawa, U. Heinz and B. Müller, *Phys. Rev. Lett.* 85 (2000) 2072; S. Jeon and V. Koch, *ibid.* 85 (2000) 2076; D. Bower and S. Gavin, *Phys. Rev.* C 64 (2001) 051902; S. Jeon, V. Koch, K. Redlich and X. N. Wang, nucl-th/0105035.

[18] Z. Fodor and S. D. Katz, *J. High Energy Phys.*, 03 (2002) 014; C. R. Allton *et al.*, hep-lat/0204010; P. de Forcrand and O. Philipsen, hep-lat/0205016; M. D'Elia and M.-P. Lombardo, hep-lat/0205022.

[19] J.-P. Blaizot, E. Iancu and A. Rebhan, *Phys. Lett.*, B 523 (2001) 143.

[20] C. DeTar and J. B. Kogut, *Phys. Rev. Lett.*, 59 (1987) 399; K. D. Born *et al.*, *Phys. Rev.*

Lett., 67 (1991) 302.

[21] S. Gottlieb *et al.*, *Phys. Rev. Lett.*, 59 (1987) 1881; C. Bernard *et al.*, *Phys. Rev.*, D 45 (1992) 3854; S. Gottlieb *et al.*, *Phys. Rev.*, D 47 (1993) 3619.

[22] A. Gocksch, P. Rossi and U. Heller, *Phys. Lett.*, B 205 (1988) 334.

[23] S. Gupta, *Phys. Lett.*, B 288 (1992) 171.

[24] G. Boyd, S. Gupta and F. Karsch, *Nucl. Phys.*, B 385 (1992) 482; G. Boyd *et al.*, *Z. Phys.*, C 64 (1994) 331, and *Phys. Lett.*, B 349 (1995) 170.

[25] R. V. Gavai, S. Gupta and R. Lacaze, *Phys. Rev.*, D 65 (2002) 094504.

[26] T. Hashimoto, A. Nakamura and I. O. Stamatescu, *Nucl. Phys.*, B 406 (1993) 325; P. de Forcrand *et al.*, *Phys. Rev.*, D 63 (2001) 054501; E. Laermann and S. Schmidt, *Eur. Phys. J.*, C 20 (2001) 541.

[27] S. Gupta, *Phys. Rev.*, D 60 (1999) 094505.

[28] S. Naik, *Nucl. Phys.*, B 316 (1989) 238.

[29] K. Symanzik, *Nucl.Phys.*, B 226 (1983) 187;

[30] P. Hasenfratz and F. Karsch, *Phys. Lett.*, B 125 (1983) 308; N. Bilic and R. V. Gavai, *Z. Phys.*, C 23 (1984) 77; R. V. Gavai, *Phys. Rev.*, D 32 (1985) 519.

[31] R. V. Gavai and S. Gupta, *Phys. Rev. Lett.*, 83 (1999) 3784.

[32] R. V. Gavai, hep-lat/0209008.

[33] A. Wroblewski, *Acta Phys. Pol.*, B 16 (1985) 379.

[34] J. Cleymans, hep-lat/0201142.

[35] Here V_μ is the polarisation μ of the $T = 0$ vector operator and AV_μ is the polarisation μ of the $T = 0$ axial vector.

[36] Equally good fits are obtained to the form $\chi_3(a)/T^2 = \chi_3/T^2(1 + s'/N_t^2)^{-1}$.

[37] Since the study in [15] used only $N_t \leq 8$, the extrapolation of χ_3/T^2 led to strong underestimation of the continuum limit. Since the extrapolation affected χ_3 and χ_s in the same way, the results for the Wroblewski parameter, λ_s, were almost unaffected, as this work verifies. The results for χ_{ud}/T^2 were unrelated, and hence unaffected.